NIH-PA Author Manuscript

NIH-PA Author Manuscript

NIH-PA Author Manuscript

Biological Evaluation of pH-Responsive Polymer-Caged Nanobins for Breast Cancer Therapy

Sang-Min Lee[†,1,3,6], **Richard W. Ahn**[†,1,3,6], **Feng Chen**[3,4,6], **Angela J. Fought**[5,6], **Thomas V. O'Halloran**[*,1,2,3,6], **Vincent L. Cryns**[*,3,4,6], and **SonBinh T. Nguyen**[*,1,3,6]

[1]Department of Chemistry, Northwestern University, 2145 Sheridan Road, Evanston, Illinois 60208

[2]Department of Biochemistry, Molecular Biology, and Cell Biology, Northwestern University, 2145 Sheridan Road, Evanston, Illinois 60208

[3]Center of Cancer Nanotechnology Excellence, Northwestern University, 2145 Sheridan Road, Evanston, Illinois 60208

[4]Departments of Medicine and Cell and Molecular Biology, Cell Death Regulation Laboratory, Northwestern University, 303 East Chicago Avenue, Chicago, Illinois 60611

[5]Department of Preventive Medicine, Feinberg School of Medicine, Northwestern University, 303 East Chicago Avenue, Chicago, Illinois 60611

[6]Robert H. Lurie Comprehensive Cancer Center, Northwestern University, 303 East Chicago Avenue, Chicago, Illinois 60611

Abstract

A series of doxorubicin-loaded polymer-caged nanobins (PCN_{DXR}) were evaluated *in vivo* in a murine MDA-MB-231 xenograft model of triple-negative breast cancer. The cross-linked polymer cage in PCN_{DXR} offers protection for the drug payload while serving as a pH-responsive trigger that enhances drug release in the acidic environments commonly seen in solid tumors and endosomes. Varying the degree of cross-linking in the polymer cage allows the surface potential of PCN_{DXR}, and thus the *in vivo* circulation lifetime of the nanocarriers, to be tuned. Given these design advantages, the present study provides the first *in vivo* evidence that PCN_{DXR} can effectively inhibit tumor growth in a murine model of breast cancer. Importantly, PCN_{DXR} was well-tolerated by mice, and drug encapsulation attenuated the toxicity of free doxorubicin. Taken together, this study demonstrates the potential utility of the PCN platform in cancer therapy.

Keywords

Liposomes; Polymers; Breast Cancer; pH-Responsive Release; In Vivo Drug Delivery

Nanoparticles have been demonstrated to provide numerous advantages as cancer drug delivery vehicles, including more favorable pharmacokinetic properties, enhanced tumor delivery, and reduced toxic side effects compared to conventional small-molecule chemotherapy.[1-3] For example, doxorubicin (DXR) encapsulated inside sterically stabilized liposomes (SSLs, ~100 nm) is used clinically for the treatment of Kaposi's sarcoma, multiple myeloma, breast and ovarian cancers.[4, 5] This formulation, marketed under the trade name Doxil® (Ortho Biotech Products, L.P., Horsham, PA), dramatically increases plasma half-life in humans (45-80 h)[6] compared to free DXR (10 h). Nano-encapsulation of DXR also enhances intratumor accumulation of DXR due to the enhanced permeation and retention (EPR) effect.[7] SSL-encapsulation of DXR prevents premature drug degradation and limits the exposure of healthy tissue to this cytotoxic agent as demonstrated by a striking reduction in cardiotoxicity compared to that for the free drug.[4, 5] In spite of these benefits, the therapeutic efficacy of current drug delivery vehicles can still be improved if triggered drug-release capability can be incorporated so that, the payload can be efficiently released at the tumor site.[8, 9]

Over the last decade, pH-sensitive lipid components,[10] such as phosphatidylethanolamine[11, 12] and acid-labile poly(ethylene glycol),[13, 14] have been used to trigger and enhance drug release by SSLs. Recently, we have developed a lipid-based, 100-nm polymer-caged nanobin (PCN) platform that combines pH-dependent drug-release with a facile click-based chemical modification for the attachment of targeting ligands or imaging agents.[15, 16] In this system, the polymer cage (Figure 1A) provides steric stability around the lipid shell and significantly reduces the leakage of drug prior to arrival at the target site, as demonstrated in an *in vitro* serum challenge.[15] The surface of the polymer cage enables drug release at low-pH target sites such as tumor interstitium[17, 18] and cellular endosomal vesicles.[12, 19] Presumably, the free carboxylate groups in the cross-linked acrylamide polymer cage are protonated in acidic environments, which results in pockets of increased local hydrophobicity on the surface of the PCN, ultimately leading to the collapse of the vesicle and the release of the drugs (Figure 1B).[15] Herein, we optimized the surface charge of the PCN platform for *in vivo* drug delivery by varying the cross-link density and demonstrated the enhanced *in vivo* therapeutic efficacy of a DXR-loaded, pH-responsive PCN (PCN_{DXR}) system in a murine model of an aggressive type of breast cancer. Moreover, PCN_{DXR} was well-tolerated even at doses above those of free DXR that result in weight loss.

Results and Discussion

DXR-loaded bare liposomes (BL_{DXR}, ~ 0.3 mol/mol drug-to-lipid ratio) were prepared by an ion gradient-mediated drug-loading process previously described.[20] PCNs were constructed from the resulting BL_{DXR} and cholesterol-terminated poly(acrylic acid) (Chol-PAA, M_n = ~ 3,700 Da) via our *drop-in* method[15] followed by *in situ* cross-linking with diamine linkers (Figure 1C). The surface charge of the PCNs can be tuned by the degree of cross-linking and evaluated using zeta potential (ζ) measurements in pH 7.4-buffered solution (Figure 2A). As expected, the negatively charged lipids in the liposome shell (3.6 mol% of phosphatidylglycerol) engenders a slightly negative ζ (–4.14 mV) on the parent BL. After insertion of Chol-PAA into the BLs, the negatively charged acrylate groups in Chol-PAA resulted in a decreased ζ to –31.3 mV. Cross-linking at 30, 50, and 70% increased ζ to –23.0, –15.1, and –11.3 mV, respectively, by conversion of free acrylates into neutral amide bridges.[21] The ζ for PCNs with more than 80% cross-linking could not be measured due to significant inter-particle cross-linking and aggregations (Figure S1 in Supporting Information (SI)). Nanoparticles, having near-neutral surface potential (–15 to 10 mV), tend to have reduced clearance *in vivo*[22,23] but excessive cross-linking, which affords more robust nanostructures[24] can hinder the release of payload. Based on our

physicochemical characterization, we selected PCNs with 50% cross-linking as the ideal system for further *physical* and *in vivo* studies with their optimal stability and release properties.

After cross-linking, the hydrodynamic diameter (D_H) of PCN_{DXR} increased to 124.5 ± 17.2 nm (mean ± standard deviation (SD)) as measured by dynamic light scattering (DLS, Figure 2B), which is ~30% larger than that of the parent BL_{DXR} (93.5 ± 15.3 nm). Compared to BL_{DXR}, the amount of DXR released from PCN_{DXR} is greatly enhanced at low pH conditions at 37 °C (Figure 2C), consistent with our previous observations.[16] More than 70% of DXR was released at pH 5.0 after 24 h with complete release occurred at 48 h. In contrast, only 50% of DXR was released from BL_{DXR} after 72 h at pH 5.0. After being incubated at pH 5.0, the PCNs loses their well-defined shapes and become irregular particles as seen by transmission electron microscopy (cf. Figures 1C and 1D), presumably due to the collapse of the vesicles induced by pH-responsive polymer-shrinkage (Figure 1B).[15] Given that the peak DXR level in malignant effusions in patients treated with Doxil are reached 3-7 days after treatment,[6] nanoparticles ideally should remain intact in serum for at least 3 days. In our bench-top release experiments, less than 20% of drug was released from PCN_{DXR} after 72 h in fetal bovine serum (FBS) (Figure 2C), suggesting that these nanobins would be stable *in vivo* (i.e., in serum) for several days, allowing continued drug uptake into tumor.

Two main contributors to the *in vivo* instability of liposome-based drug delivery vehicles are lipid mixing and membrane fusion, both of which result in drug leakage.[11, 14] As these phenomena change the liposome size distribution, they can be best monitored using DLS as the apparent rate of change (k^σ) in standard deviation (σ) of vesicle diameters.[25, 26] The enhanced stability of PCNs, which is a result of the steric stabilization by the cross-linked polymer cage, is clearly evidenced by a small k^σ_{PCN} (0.04 h^{-1}) in pH 7.4-buffered saline (Figure 2D). In contrast, the apparent rate of change for BL (k^σ_{BL} =0.4h^{-1}) is ten fold higher, consistent with the rapid lipid exchange as previously demonstrated in BLs.[27]

The *in vitro* cytotoxicity of PCN_{DXR} was evaluated against multiple human cancer cell lines: MDA-MB-231 basal-like breast cancer and HeLa cervical cancer. Cells were treated with PCN_{DXR}, BL_{DXR}, free DXR, or empty PCNs for either 48 h or 72 h and the percentage of viable cells was determined by MTS assay.[28] For comparison, empty PCNs (i.e., PCN loaded with only HEPES-buffered saline), BL_{DXR} (Figure S2 in SI), and free DXR were simultaneously evaluated. The relative dose-responsive cell viability percentages compared to the drug-free control (media only) were plotted against the total DXR concentration (Figure 3). The half maximal inhibitory concentration (IC_{50}) of PCN_{DXR} against MDA-MB-231 cells (Figure 3A and Table 1) was 29.6 ± 7.7 µg/mL after 48-h incubation and 6.2 ± 1.2 µg/mL after 72-h treatment, while the IC_{50} of free DXR was 8.4 ± 1.4 at 48 h and 1.4 ± 0.7 at 72 h. Similar trends were observed in HeLa cells (Figure 3B and Table 1). Our findings are consistent with the attenuated cytotoxicity of drug-encapsulated liposome formulations compared to free drug.[16, 29] No significant cytotoxicity was observed with empty PCNs at lipid concentrations up to 1.5 mM in either cell line. To further evaluate the selectivity of the PCN_{DXR} for cancer cells, we treated immortalized human mammary epithelial cells (MCF-10A vector, non-cancer control) and transformed MCF-10A-H-RasV12 cells (i.e., MCF-10A cells stably transduced with the H-RasV12 oncogene to make them cancerous) with PCN_{DXR} (0, 1, 10 µM DXR).[30] We found that the PCN_{DXR} at 10 µM induced 2.2-fold increased cell death (defined by Annexin V-positivity) in the cancerous cell line compared to the control cells (Figure 4). This result demonstrates that cancer cells are more susceptible to PCN_{DXR}-induced cell death than non-cancer cells.

The reduced cytotoxicity of PCN_{DXR}, in contrast to the potent activity of free DXR, in MDA-MB-231 breast carcinoma cells suggests that PCN_{DXR} would be effective at both

controlling tumor growth and reducing systemic toxicities if it could be delivered to the tumor and selectively released. Hence we evaluated the *in vivo* therapeutic efficacy of PCN_{DXR} in female athymic nude mice bearing orthotopic tumors in the 4th mammary fat pad established from MDA-MB-231 triple-negative breast carcinoma (TNBC) cells.[31] Triple-negative, or basal-like, tumors are categorized by the absence of estrogen receptor, progesterone receptor, and human epidermal growth factor receptor 2 (HER2/ErbB2).[32] TNBC is thus refractory to both endocrine therapy and Herceptin™, the most effective targeted treatments for breast cancer developed to date.[33] We postulated that our PCN delivery platform would provide a novel therapeutic opportunity for this intractable disease. To this end, we bilaterally injected female nude mice with mCherry-labeled MDA-MB-231 cells (1.0×10^6 cells) into the duct of the 4th mammary fat pad. The fluorescent 'mCherry' label is an engineered, monomeric red-fluorescent protein (mRFP),[34, 35] which enables non-invasive fluorescent imaging of mammary tumors.[36] After tumors were established, mice (n = 3 mice with bilateral tumors, 6 tumors per group) were treated with PCN_{DXR} (2.0 mg DXR/kg), free DXR (2.0 mg DXR/kg), or empty PCN vehicles, by intraperitoneal injection once a week for a total of four doses over three weeks.[37]

The tumor growth rates were compared between the three groups over time using a random effects mixed model including an interaction.[38] There was a statistically significant difference in tumor growth rates between the treatment groups over time (interaction p < 0.01). Post-hoc pairwise comparisons between the three groups were also performed at each measurement and Bonferroni-corrected. The mammary tumors in mice treated with PCN_{DXR} were significantly smaller than those treated with empty PCNs beginning at week 2 of the study (Figure 5A) and free DXR on weeks 1.5 and 2.5 (not displayed in Figure 5A). Although there was a trend towards smaller tumors in mice treated with free DXR compared to mice treated with empty PCNs, these differences were not statistically significant (for complete statistical details see SI). Taken together, these results indicate that PCN_{DXR} inhibited mammary tumor growth *in vivo*, while the corresponding dose of free DXR did not significantly reduce tumor burden in this model. Indeed, PCN_{DXR} treatment resulted in ~75% reduction in tumor burden at the end of the study (Figure 5A). The treatments were well-tolerated as no statistically significant weight loss was observed in any of the treatment groups, suggesting little systemic toxicity (Figure 5B). Primary tumor burden was also assessed by whole-animal fluorescent imaging, which revealed visibly smaller tumors in mice treated with PCN_{DXR} compared to the other two treatment groups, further supporting superior therapeutic efficacy of PCN_{DXR} (Figure 6).

We also evaluated higher doses of PCN_{DXR} in animals with greater tumor burden. Using the aforementioned MDA-MB-231 xenograft model, mice were administered a PBS control; 2.0, 5.0, or 7.5 mg DXR/kg of PCN_{DXR} for three weeks. In this experiment, mammary tumors were allowed to grow to larger size (~ 200% of the tumor size in the first study) prior to the start of treatment, which provides a more advanced tumor model. Although random effects mixed models indicated that the rates of tumor growth over time were not significantly different for the four groups (interaction p = 0.21), post-hoc pairwise comparisons among the groups (Bonferroni-corrected) showed a statistically significant difference in tumor volumes between the two higher doses, 5.0 and 7.5 mg DXR/kg, and PBS, beginning at day 12 (Figure 7A). PCN_{DXR} at the 2.0 mg DXR/kg dose was significantly different from PBS on days 12 and 15 (not shown in Figure 7A, for complete statistical details see SI). Most importantly, all PCN_{DXR} treatments were well-tolerated without observable weight loss at the increased doses or observed toxicities (Figure 7B). This is in stark contrast to free DXR in this murine model, which caused significant weight loss at 5.0 mg DXR/kg (data not shown). Although this study was terminated early due to tumor ulceration, these experiments suggest that the PCN platform is effective at attenuating

the systemic toxicity of DXR *in vivo*, enabling higher doses to be administered to enhance therapeutic efficacy.

Conclusion

In summary, we have demonstrated that PCN-encapsulation of DXR potentiates the antitumor activity of DXR *in vivo* and attenuates the systemic toxicity compared to the free drug. Encapsulation of the highly toxic chemotherapeutic agent DXR in the PCN allows for higher doses of DXR to be administered to mice, thereby augmenting its therapeutic efficacy without causing weight loss or apparent toxicities during the course of treatment. Moreover, PCN_{DXR} is more cytotoxic to cancer cells in culture than non-cancer cells, further supporting its potential utility as a cancer therapeutic agent. Because the PCN *drop-in* technology can be used with virtually any lipid composition without hampering the encapsulated drug, the encapsulated cargo can be expanded to include diverse anticancer agents such as arsenic trioxide[29] and cisplatin.[39] Therapeutic efficacy can likely be further enhanced by active targeting, achievable via biocompatible, click-based conjugation onto the PCN shell.[16] These modifications should allow for precise and efficient delivery of cytotoxic agents to tumors. Future studies will investigate the effects of tumor targeting as well as optimizing dose and schedule to further enhance the antitumor activity of the PCN platform.

Materials and Methods

Materials

Unless otherwise noted, all reagents and materials were purchased from commercial sources and used as received. 1,2-dipalmitoyl-sn-glycero-3-phosphocholine (DPPC) and 1,2-dioleoyl-sn-glycero-3-[phospho-rac-(1-glycerol)] (sodium salt) (DOPG) were purchased from Avanti Polar Lipids (Alabaster, AL). Doxorubicin is purchased from Polymed Therapeutics, Inc. (Houston, TX). ICP calibration standard solutions of phosphorus (1000 μg/mL P), 1-(3-dimethylaminopropyl)-3-ethylcarbodiimide methiodide (EDC·MeI), and all other reagents were purchased from Aldrich Chemical Company (Milwaukee, WI). Tert-butyl acrylate was stirred over CaH2 under nitrogen and fractionated by vacuum transfer right before use. Cholesterol-terminated poly(acrylic acid) was prepared using a literature procedure.[15] Ultrapure deionized water was obtained from a Millipore system (18.2 MΩ cm resistivity).

Measurements

Fourier-transformed nuclear magnetic resonance (NMR) spectroscopy was performed on a Varian INOVA-500 MHz spectrometer in the Northwestern Integrated Molecular Structure Education and Research Center (IMSERC) facilities. Chemical shifts of ^1H NMR spectra are reported in ppm against residual solvent resonance as the internal standard ($CHCl_3$ = 7.27 ppm, CHD_2COCD_3 = 2.05 ppm, CHD_2OD = 3.31 ppm). Fluorescence emission spectra were obtained on a Jobin Yvon Fluorolog fluorometer (λ_{ex} = 475 nm, λ_{em} = 596 nm, slith width = 3 nm for doxorubicin). UV-vis absorption spectra were obtained on a CARY 300 Bio UV-vis spectrophotometer.

Electrospray-ionization mass spectrometric (ESIMS) data were obtained on a Micromass Quattro II triple quadrupole mass spectrometer. Phosphorus concentration was determined using a Varian Vista MPX simultaneous inductively coupled plasma optical emission spectrometer (ICP-OES).

Polymer molecular weights were measured relative to polystyrene standards on a Waters gelpermeation chromatograph (GPC) equipped with Breeze software, a 717 autosampler,

Shodex KF-G guard column, KF-803L and KF-806L columns in series, a Waters 2440 UV detector, and a 410 RI detector. HPLC-grade THF was used as an eluent at a flow rate of 1.0 mL/min and the instrument was calibrated using polystyrene standards (Aldrich, 15 standards, 760-1,800,000 Daltons).

Zeta potential and dynamic light scattering (DLS) measurements were performed on a Zetasizer Nano ZS (Marvern Instruments, Malvern, UK) with a He-Ne laser (633 nm). Non-invasive backscatter method (detection at 173° scattering angle) was used. Correlation data were fitted, using the method of cumulants, to the logarithm of the correlation function, yielding the diffusion coefficient, D. The hydrodynamic diameters (D_H) of the BLs and PCNs were calculated using D and the Stokes-Einstein equation ($D_H = k_B T/3\pi\eta D$, where k_B is the Boltzmann constant, T is the absolute temperature, and η is the solvent viscosity ($\eta =$ 0.8872 cP for water)). The polydispersity index (PDI) of liposomes— represented as $2c/b^2$, where b and c are first and second order coefficients, respectively, in a polynomial of a semi-log correlation function—was calculated by the cumulants analysis. Size distribution of vesicles was obtained by the non-negative least squares (NNLS) analysis. Unless noted otherwise, all samples were dispersed in 10-mM HEPES solution (pH 7.4, 150 mM NaCl) for DLS measurements. The data reported represent an average of ten measurements with five scans each.

Preparation of Doxorubicin-loaded Polymer-Caged Nanobins

Doxorubicin-loaded bare liposome was prepared using a modified literature procedure.[20] DPPC (108.29 μmol), DOPG (6.91 μmol), and cholesterol (76.8 μmol, 40 mol% of the total membrane components; this number is chosen to eliminate the thermal instability of the liposomes that is attributable to the intrinsic phase-transition temperature of the lipid) were added to a 20-mL cylindrical glass vial, followed by chloroform (5 mL) to make a colorless solution. After vortexing (~1 min), the solvent was removed by passing a stream of nitrogen over the solution while the vial was warmed in a 50 °C water bath. The resulting dry film was further dried under vacuum on a Schlenk line (< 30 mTorr) over night. Next, the dry lipid films were hydrated in 300 mM aqueous ammonium sulfate solution (5 mL) followed by vigorous vortexing (3-5 min on a Vortex Mixer, American Scientific Products) to form a dispersion of multilamellar vesicles. After this dispersion was subjected to 10 freeze-thaw cycles, it was extruded ten times through two stacked polycarbonate extrusion membranes (100-nm pore-size) that are maintained at 50 °C in a LIPEX™ extruder (Northern Lipids Inc., Burnaby, BC, Canada). The excess ammonium sulfate outside liposome was removed by Sephadex G-50 (50 mL) gel-filtration chromatography pre-equilibrated with 150-mM NaCl solution.

Doxorubicin (DXR, 0.32 equiv of the total lipid content) was added to the collected liposome solution (~7-10 mL of a solution with ~4-mM lipid concentration) and incubated at 50 °C for 24 h. The excess DXR outside of the liposome was then removed by Dowex 50WX4 cation-exchange resin (20 mL). The loading of the DXR was determined by breaking up the DXR-loaded liposome in a 75 mM HCl solution in 2-propanol/water (9/1 v/ v) and measuring the dissolved doxorubicin concentration using UV-vis spectroscopy based on the extinction coefficient (ε) of DXR (11207 $M^{-1}cm^{-1}$ at $\lambda_{max} =$ 480 nm). Mean hydrodynamic diameter (D_H) of 93.5 ± 15.3 nm was determined by DLS measurements.

The DXR-loaded bare liposomes (BL$_{DXR}$) were next subjected to the PCN fabrication process as reported previously.[15] For this process, 10 mol% of the Chol-PAA modifier was chosen to maximize the amount of the modifier. Additionally, 30, 50, and 70% of acrylate repeating units in Chol-PAA chains were cross-linked with diamine linker (15, 25, and 35 mol%; if >35 mol% of the cross-linker is used, precipitation will occur, due to interparticle cross-linking, Figure S1). The mean D_H of the PCN (124.5 ± 17.2 nm) was determined by

DLS measurements as described in the Measurements section. After the purification by Sephadex G-50 column, the resulting DXR-loaded PCN (PCN_{DXR}) can be used directly for further study. To determine the final concentration of DXR in the as-prepared PCN_{DXR}, an aliquot of the solution was broken up with reduced Triton X-100 (5 vol% aqueous solution). The dissolved doxorubicin concentration was then measured using UV-vis spectroscopy based on the extinction coefficient (ε) of free DXR at known isosbestic point[40] (3530.6 $M^{-1}cm^{-1}$ at $\lambda = 543$ nm).

DXR-Release Assay under Various pH Conditions (Figure 2C)

Solutions of BL_{DXR} and PCN_{DXR} (1.0 mM of lipids)—each in 20 mM acetate buffer (pH 5.0, 150 mM NaCl), 20 mM MES buffer (pH 6.0, 150 mM NaCl), and fetal bovine serum (FBS)—were incubated in a 3-mL quartz fluorescence cell (Hellma Cells Inc., Plainview, NY) at 37 °C with magnetic stirring. The fluorescence from the liposome-encapsulated DXR was significantly self-quenched due to its high concentration inside the liposome.[15] Hence, only the fluorescence from the DXR that has released out of the liposome was measured as a function of incubation time. Afterward, 5% aqueous Triton X-100 (reduced form) was added to totally break up the liposomes and the final DXR fluorescence was measured to give the 100% release value. The extent of release was observed by comparing to the maximum release value.

Cell Culture

a. Medium—Eagle's Minimum Essential Medium (EMEM) was purchased from ATCC (Manassas, VA). Trypsin solution (0.25%, containing EDTA) was purchased from Invitrogen (San Diego, CA). Penicillin-Streptomycin and phosphate-buffered saline (PBS, 1× without calcium and magnesium) solutions were purchased from Mediatech (Manassas, VA).

b. Cell Lines—Human triple-negative MDA-MB-231 basal-like breast cancer cells and HeLa cervical cancer cells were continuously cultured in EMEM supplemented with 10 vol% heat-inactivated fetal bovine serum (FBS) and 0.5 vol% Penicillin-Streptomycin solution at 37 °C in a humidified atmosphere containing 5% CO_2. MCF-10A cells stably expressing H-RasV12 or empty vector were cultured in phenol red-free DMEM/F12 with 5 vol% heat-inactivated horse serum, insulin (10 µg/mL), EGF (20 ng/mL), cholera toxin (100 ng/mL), and hydrocortisone (0.5 µg/mL) at 37 °C in a humidified atmosphere containing 5% CO_2.[29]

Cytotoxicity Assays

(Figure 3) Either MDA-MB-231 or HeLa cells were seeded in 96-well plates (100 µL/well) at a concentration of 100,000 cells/mL in EMEM and were incubated for 24 h. At that point, the media in the wells were replaced with a pre-prepared growth media containing the appropriate drug formulation in EMEM (100 µL of solution at the appropriate doxorubicin concentrations). The drug-treated cells were further incubated for either 48 or 72 h in a humidified atmosphere containing 5% CO_2 at 37 °C, after which time the cells were washed with PBS buffer (2×150 µL). The percentage of viable cells was determined by MTS assay[28] and the relative cell survival percentages compared to the drug-free control were plotted against the total DXR concentration in logarithmic scale. The data reported represent an average of three measurements from different batches. The dose-response curves were obtained by sigmoidal logistic fitting using *Origin* software (version 6.1, OriginLab Corp., Northampton, MA) and the half maximal inhibitory concentration (IC_{50}) values were determined on the basis of the fitted data.

Apoptosis Assay

Apoptosis was measured by fluorescence-activated cell sorting (FACS) using annexin-V, Alexa Fluor® 647 conjugate (Invitrogen, Carlsbad, CA) as apoptosis indicator and 4′,6-diamidino-2-phenylindole (DAPI) as a dead cell indicator, following the manufacturer's protocol. Cells were treated with PCN_{DXR} (1 or 10 μM) for 48 h prior to analysis at the Robert H. Lurie Cancer Center Flow Cytometry Core Facility. The data was plotted with the horizontal axis in each plot representing the Annexin-V fluorescent intensity in log scale and the vertical axis of each plot representing the DAPI fluorescent intensity in log scale. The color dots represent histogram of cells that exhibit a particular combination of Annexin-V/ DAPI fluorescence; a dot with brighter color indicates a higher number of cells in that fluorescence category (red > yellow > green > blue, etc.).

In Vivo Therapeutic efficacy Study

Mammary tumors were measured twice weekly with a caliper and the tumor volume was calculated using the formula $VTumor = (w^2 \times l \times \pi)/6$); w = minimal width, l = maximum length. Mice were weighed weekly and their tumor volumes were plotted using *GraphPad Prism* software (Version 5, GraphPad Software, Inc., La Jolla, CA) (Figures 5 and 7). All animal experiments were conducted under protocols approved by the Animal Care and Use Committee of Northwestern University. SAS® version 9.2 (Cary, NC) was used to generate Models A, B1-12, C, and D1-6 (vide infra).

a. Tumor Inoculation—Human triple-negative MDA-MB-231 cells suspended in chilled Matrigel (BD Biosceince, Bedford, MA) were injected bilaterally into the lactiferous ducts of the 4th mammary gland (1×10 cells/200 uL injection) of female athymic nu/nu mice (Harlan, Indianapolis, IN) that are 5-6 weeks old.

b. Efficacy Study 1—Twelve days after tumor implantation, mice were randomly assigned to PCNdxr (2.0 mg/kg), empty PCNs, or free DXR (2.0 mg DXR/kg) groups and given weekly intraperitoneal injections for four weeks. At the end of the study, mice were sacrificed and imaged using an Olympus OV-100 Small Animal Imaging System. Fluorescent images were pseudocolored using ImageJ software (Version 1.42, NIH, Bethesda, MD) and overlayed using Adobe Photoshop (CS3, Adobe Systems, San Jose, CA). Uniform CCD gain and lamp intensity were used for all images.

c. Efficacy Study 2—Ten days after tumor implantation, mice were randomly assigned to PCN_{DXR} (2.0, 5.0, and 7.5 mg DXR/kg), and PBS groups and each drug formulation or PBS were given weekly intraperitoneal injections for three weeks.

Statistical Analysis of Efficacy Study 1

The differences between the treatment groups over the twelve time points were tested using linear mixed models with treatment group and time as the fixed effects, a treatment by time interaction, and a random effect for each tumor, using a significance level of $\alpha = 0.05$. This tests if there is a different rate of tumor growth over time. Post-hoc pairwise comparisons of the treatment groups were also performed using Bonferroni-adjusted p-values (Figure 5A, Table S1 in SI).

Statistical Analysis of Efficacy Study 2

Differences among the four groups were tested using linear mixed models with the treatment group and time as fixed effects, a treatment by time interaction, and a random time effect for each tumor, again using a significance level $\alpha = 0.05$. Post-hoc pairwise comparisons of the

four treatment groups were also performed, using Bonferroni-adjusted p-values (Figure 7A, Table S2 in SI).

Supplementary Material

Refer to Web version on PubMed Central for supplementary material.

Acknowledgments

References and Notes

1. Allen TM, Cullis PR. Drug Delivery Systems: Entering the Mainstream. Science. 2004; 303:1818–1822. [PubMed: 15031496]

2. Peer D, Karp JM, Hong S, Farokhzad OC, Margalit R, Langer R. Nanocarriers as an Emerging Platform for Cancer Therapy. Nat Nanotechnol. 2007; 2:751–760. [PubMed: 18654426]

3. Davis ME, Chen Z, Shin DM. Nanoparticle Therapeutics: An Emerging Treatment Modality for Cancer. Nat Rev Drug Discov. 2008; 7:771–782. [PubMed: 18758474]

4. Drummond DC, Meyer O, Hong K, Kirpotin DB, Papahadjopoulos D. Optimizing Liposomes for Delivery of Chemotherapeutic Agents to Solid Tumors. Pharmacol Rev. 1999; 51:691–744. [PubMed: 10581328]

5. Waterhouse DN, Tardi PG, Mayer LD, Bally MB. A Comparison of Liposomal Formulations of Doxorubicin with Drug Administered in Free Form: Changing Toxicity Profiles. Drug Saf. 2001; 24:903–920. [PubMed: 11735647]

6. Gabizon A, Catane R, Uziely B, Kaufman B, Safra T, Cohen R, Martin F, Huang A, Barenholz Y. Prolonged Circulation Time and Enhanced Accumulation in Malignant Exudates of Doxorubicin Encapsulated in Polyethylene-Glycol Coated Liposomes. Cancer Res. 1994; 54:987–992. [PubMed: 8313389]

7. Maeda H, Wu J, Sawa T, Matsumura Y, Hori K. Tumor Vascular Permeability and the EPR Effect in Macromolecular Therapeutics: A Review. J Control Release. 2000; 65:271–284. [PubMed: 10699287]

8. Bandak S, Goren D, Horowitz A, Tzemach D, Gabizon A. Pharmacological Studies of Cisplatin Encapsulated in Long-Circulating Liposomes in Mouse Tumor Models. Anti-Cancer Drugs. 1999; 10:911–920. [PubMed: 10630359]

9. Laginha KM, Verwoert S, Charrois GJR, Allen TM. Determination of Doxorubicin Levels in Whole Tumor and Tumor Nuclei in Murine Breast Cancer Tumors. Clin Cancer Res. 2005; 11:6944–6949. [PubMed: 16203786]

10. Rui Y, Wang S, Low PS, Thompson DH. Diplasmenylcholine-Folate Liposomes: An Efficient Vehicle for Intracellular Drug Delivery. J Am Chem Soc. 1998; 120:11213–11218.

11. Connor J, Yatvin MB, Huang L. pH-Sensitive Liposomes: Acid-Induced Liposome Fusion. Proc Natl Acad Sci U S A. 1984; 81:1715–1718. [PubMed: 6584905]

12. Gerasimov OV, Boomer JA, Qualls MM, Thompson DH. Cytosolic Drug Delivery Using pH- and Light-Sensitive Liposomes. Adv Drug Deliv Rev. 1999; 38:317–338. [PubMed: 10837763]

13. Zalipsky S, Qazen M, Walker JA, Mullah N, Quinn YP, Huang SK. New Detachable Poly(Ethylene Glycol) Conjugates: Cysteine-Cleavable Lipopolymers Regenerating Natural Phospholipid, Diacyl Phosphatidylethanolamine. Bioconjugate Chem. 1999; 10:703–707.

14. Bergstrand N, Arfvidsson MC, Kim JM, Thompson DH, Edwards K. Interactions between pH-Sensitive Liposomes and Model Membranes. Biophys Chem. 2003; 104:361–379. [PubMed: 12834854]

15. Lee SM, Chen H, Dettmer CM, O'Halloran TV, Nguyen ST. Polymer-Caged Lipsomes: A pH-Responsive Delivery System with High Stability. J Am Chem Soc. 2007; 129:15096–15097. [PubMed: 17999499]

16. Lee SM, Chen H, O'Halloran TV, Nguyen ST. 'Clickable' Polymer-Caged Nanobins as a Modular Drug Delivery Platform. J Am Chem Soc. 2009; 131:9311–9320. [PubMed: 19527027]

17. Tannock IF, Rotin D. Acid pH in Tumors and Its Potential for Therapeutic Exploitation. Cancer Res. 1989; 49:4373–4384. [PubMed: 2545340]

18. Vaupel P, Kallinowski F, Okunieff P. Blood Flow, Oxygen and Nutrient Supply, and Metabolic Microenvironment of Human Tumors: A Review. Cancer Res. 1989; 49:6449–6465. [PubMed: 2684393]

19. Casey JR, Grinstein S, Orlowski J. Sensors and Regulators of Intracellular pH. Nat Rev Mol Cell Biol. 2010; 11:50–61. [PubMed: 19997129]

20. Haran G, Cohen R, Bar LK, Barenholz Y. Transmembrane Ammonium Sulfate Gradients in Liposomes Produce Efficient and Stable Entrapment of Amphipathic Weak Bases. Biochim Biophys Acta. 1993; 1151:201–215. [PubMed: 8373796]

21. Ma Q, Remsen EE, Kowalewski T, Wooley KL. Two-Dimensional, Shell-Cross-Linked Nanoparticle Arrays. J Am Chem Soc. 2001; 123:4627–4628. [PubMed: 11457260]

22. Li SD, Huang L. Pharmacokinetics and Biodistribution of Nanoparticles. Mol Pharm. 2008; 5:496–504. [PubMed: 18611037]

23. Vonarbourg A, Passirani C, Saulnier P, Benoit JP. Parameters Influencing the Stealthiness of Colloidal Drug Delivery Systems. Biomaterials. 2006; 27:4356–4373. [PubMed: 16650890]

24. Sun G, Hagooly A, Xu J, Nystrom AM, Li Z, Rossin R, Moore DA, Wooley KL, Welch MJ. Facile, Efficient Approach to Accomplish Tunable Chemistries and Variable Biodistributions for Shell Cross-Linked Nanoparticles. Biomacromolecules. 2008; 9:1997–2006. [PubMed: 18510359]

25. Chong CS, Colbow K. Light Scattering and Turbidity Measurements on Lipid Vesicles. Biochim Biophys Acta. 1976; 436:260–282. [PubMed: 1276217]

26. Schurtenberger P, Hauser H. Characterization of the Size Distribution of Unilamellar Vesicles by Gel Filtration, Quasi-Elastic Light Scattering and Electron Microscopy. Biochim Biophys Acta. 1984; 778:470–480.

27. Silvius JR, Leventis R. Spontaneous Interbilayer Transfer of Phospholipids: Dependence of Acyl Chain Composition. Biochemistry. 2002; 32:13318–13326. [PubMed: 8241188]

28. Barltrop JA, Owen TC, Cory AH, Cory JG. 5-(3-Carboxymethoxyphenyl)-2-(4,5-Dimethylthiazolyl)-3-(4-Sulfophenyl)Tetrazolium, Inner Salt (MTS) and Related Analogs of 3-(4,5-Dimethylthiazolyl)-2,5-Diphenyltetrazolium Bromide (MTT) Reducing to Purple Water-Soluble Formazans as Cell-Viability Indicators. Bioorg Med Chem Lett. 1991; 1:611–614.

29. Chen H, MacDonald RC, Li S, Krett NL, Rosen ST, O'Halloran TV. Lipid Encapsulation of Arsenic Trioxide Attenuates Cytotoxicity and Allows for Controlled Anticancer Drug Release. J Am Chem Soc. 2006; 128:13348–13349. [PubMed: 17031934]

30. Moyano JV, Evans JR, Chen F, Lu M, Werner ME, Yehiely F, Diaz LK, Turbin D, Karaca G, Wiley E, Nielsen TO, Perou CM, Cryns VL. Ab-Crystallin Is a Novel Oncoprotein That Predicts Poor Clinical Outcome in Breast Cancer. J Clin Invest. 2006; 116:261–270. [PubMed: 16395408]

31. Neve RM, Chin K, Fridlyand J, Yeh J, Baehner FL, Fevr T, Clark L, Bayani N, Coppe JP, Tong F, Speed T, Spellman PT, DeVries S, Lapuk A, Wang NJ, Kuo WL, Stilwell JL, Pinkel D, Albertson DG, Waldman FM, McCormick F, Dickson RB, Johnson MD, Lippman M, Ethier S, Gazdar A, Gray JW. A Collection of Breast Cancer Cell Lines for the Study of Functionally Distinct Cancer Subtypes. Cancer Cell. 2006; 10:515–527. [PubMed: 17157791]

32. Cleator S, Heller W, Coombes RC. Triple-Negative Breast Cancer: Therapeutic Options. Lancet Oncol. 2007; 8:235–244. [PubMed: 17329194]

33. Yehiely F, Moyano JV, Evans JR, Nielsen TO, Cryns VL. Deconstructing the Molecular Portrait of Basal-Like Breast Cancer. Trends Mol Med. 2006; 12:537–544. [PubMed: 17011236]

34. Shaner NC, Campbell RE, Steinbach PA, Giepmans BNG, Palmer AE, Tsien RY. Improved Monomeric Red, Orange and Yellow Fluorescent Proteins Derived from Discosoma Sp. Red Fluorescent Protein. Nat Biotech. 2004; 22:1567–1572.

35. Wang L, Jackson WC, Steinbach PA, Tsien RY. Evolution of New Nonantibody Proteins Via Iterative Somatic Hypermutation. Proc Natl Acad Sci U S A. 2004; 101:16745–16749. [PubMed: 15556995]

36. Hoffman RM. The Multiple Uses of Fluorescent Proteins to Visualize Cancer in Vivo. Nat Rev Cancer. 2005; 5:796–806. [PubMed: 16195751]

37. All animal experiments were performed in accordance with protocols approved by the Northwestern University Animal Care and Use Committee.

38. Littell RC, Henry PR, Ammerman CB. Statistical Analysis of Repeated Measures Data Using SAS Procedures. J Anim Sci. 1998; 76:1216–1231. [PubMed: 9581947]

39. Chen H, Pazicni S, Krett NL, Ahn RW, Penner-Hahn JE, Rosen ST, O'Halloran TV. Coencapsulation of Arsenic- and Platinum-Based Drugs for Targeted Cancer Treatment. Angew Chem Int Ed. 2009; 48:9295–9299.

40. Chaires JB, Dattagupta N, Crothers DM. Selfassociation of Daunomycin. Biochemistry. 1982; 21:3927–3932. [PubMed: 7126523]
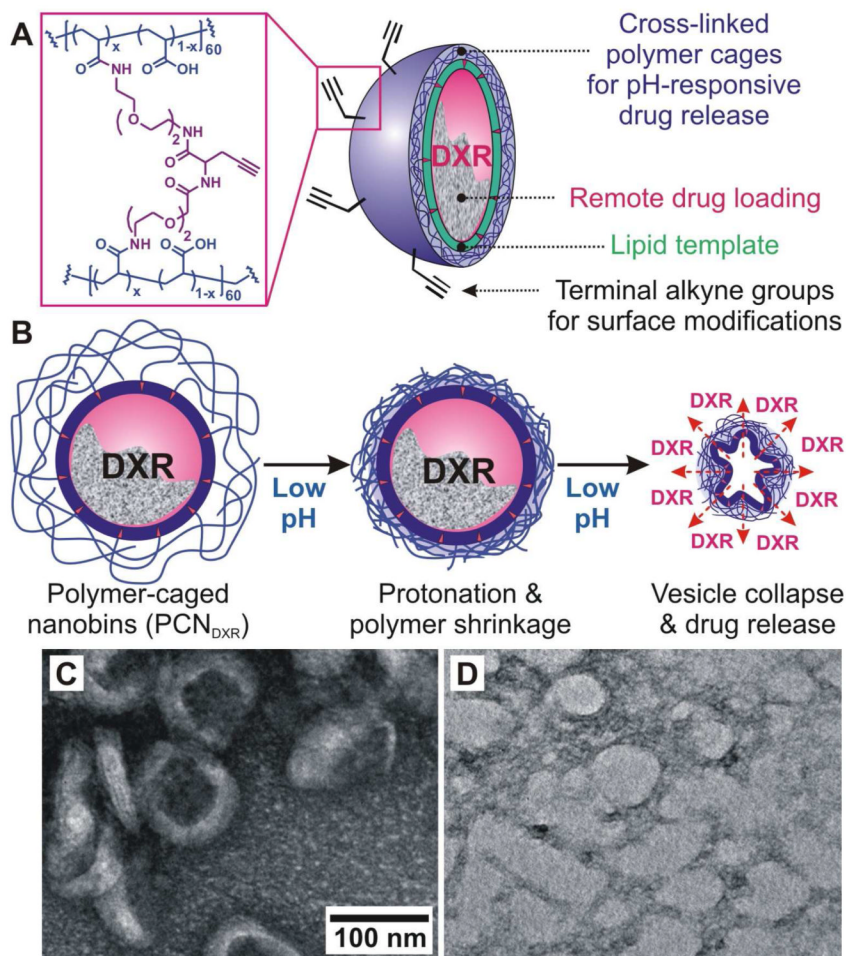
Figure 1.
(A) Schematic drawing of click-modifiable, DXR-encapsulated polymer-caged nanobins (PCN$_{DXR}$). (B) Schematic drawing of the proposed acid-triggered drug release mechanism. (C-D) Transmission electron microscopy (TEM) image of (C) intact PCNs at pH 7.4 and (D) PCNs after 72 h-incubation in pH 5.0-buffered solution at 37 °C. Both samples are stained with aqueous uranyl acetate (4 wt%) for TEM measurements.
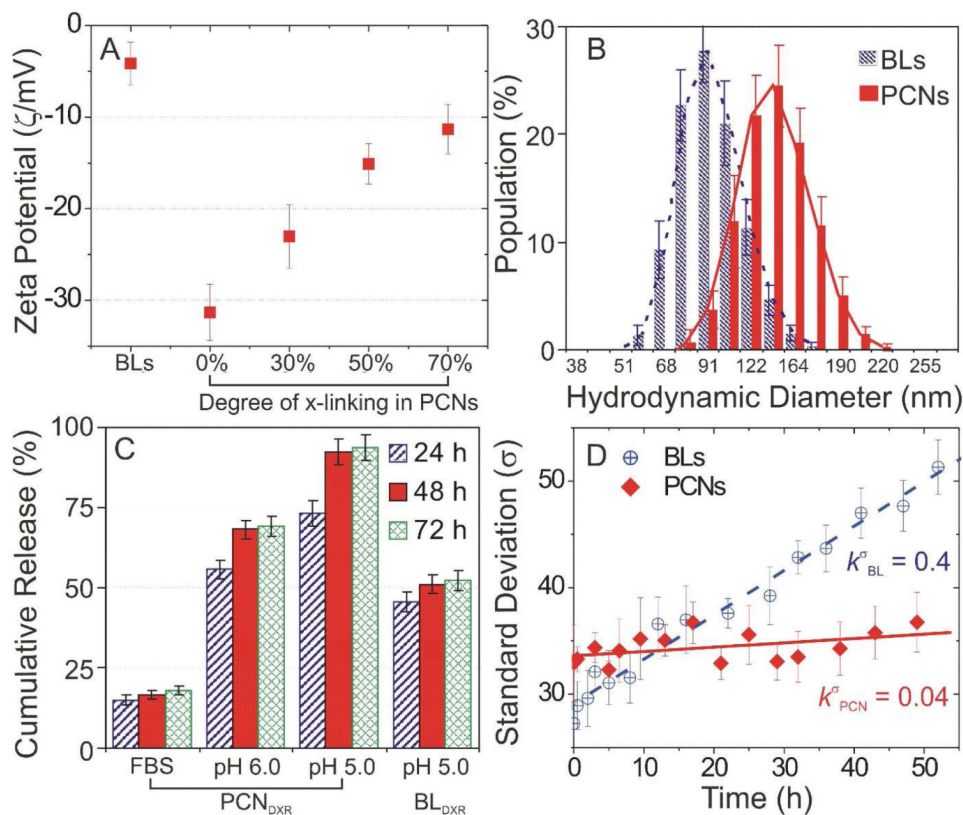
Figure 2.
(A) Zeta potentials (ζ) of doxorubicin-loaded bare liposome (BL$_{DXR}$) and polymer-caged nanobin (PCN$_{DXR}$) with 0, 30, 50, and 70% degree of cross-linking (*points*, mean ζ; *error bars*, standard deviation). (B) Hydrodynamic diameters of BL$_{DXR}$ and PCN$_{DXR}$ (50% cross-linked) measured by dynamic light scattering (*points*, mean population; *error bars*, standard deviation). (C) Cumulative amount of DXR released from PCN$_{DXR}$ (50% cross-linked) and BL$_{DXR}$ at 37 °C in fetal bovine serum (FBS) and buffered saline (pH 6.0 and 5.0) (*points*, mean value; *error bars*, standard deviation). (D) Standard deviation (SD, σ) for the diameters of BL$_{DXR}$ and PCN$_{DXR}$ (50% cross-linked) incubated at pH 7.4 (*points*, mean value; *error bars,* standard deviation).
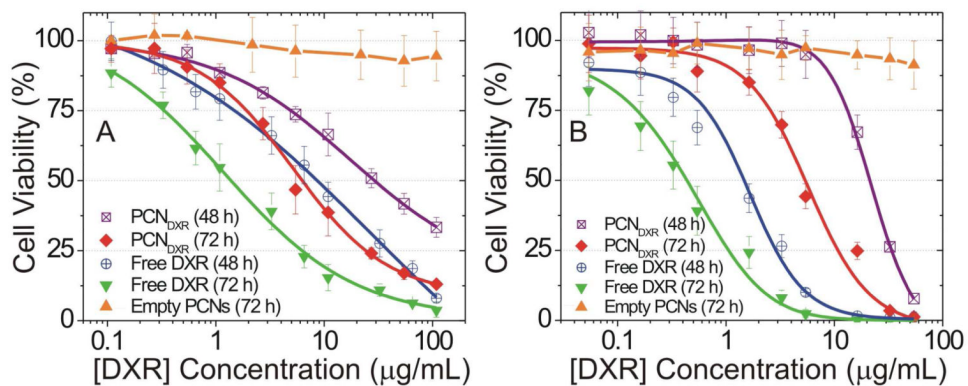
Figure 3.
In vitro cytotoxicity of DXR-encapsulated polymer-caged nanobins (PCN$_{DXR}$), empty PCN vehicles, or free DXR against (A) MDA-MB-231 and (B) HeLa cells during 48-h (open symbols) and 72-h (closed symbols) incubations. The concentration of the empty PCN vehicle was equivalent to the lipid concentration in the PCN$_{DXR}$ (*points,* mean viability; *error bars,* standard deviation).
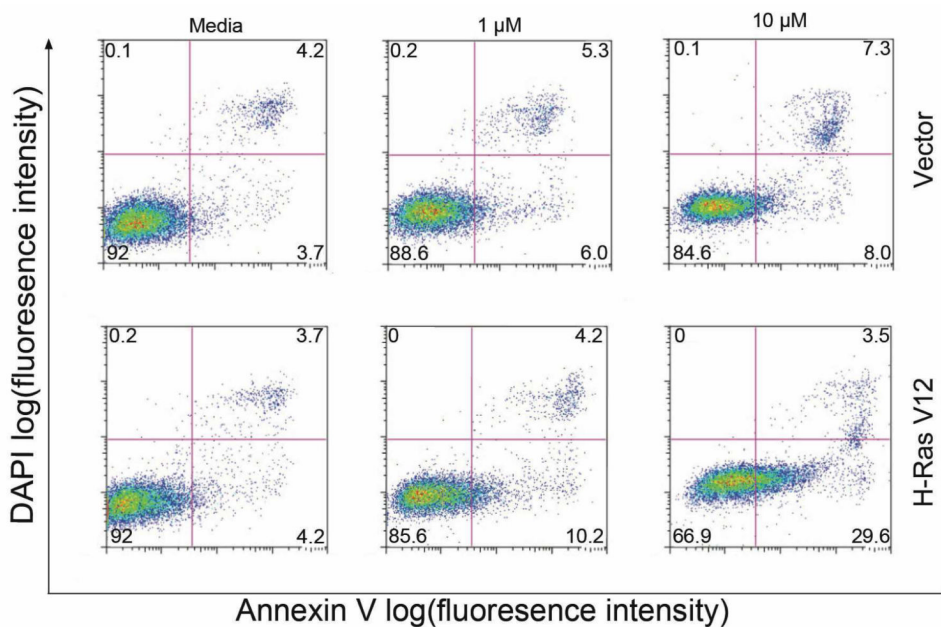
Figure 4.
Cell death induced by PCN_{DXR}, was measured by Annexin-V/DAPI staining. In each panel, the lower-left (Annexin-V$^-$, DAPI$^-$), lower-right (Annexin-V$^+$, DAPI$^-$), and upper-right (Annexin-V$^+$, DAPI$^+$) quadrants represent the populations of live cells, apoptotic cells, and necrotic/dead cells, respectively. The average %-population in each quadrant is indicated by the numbers at the corners of the panels. This data show that non-transformed MCF-10A breast epithelial cells stably expressing empty vector (i.e., control cells) were less sensitive than MCF-10A cells stably transduced with the H-RasV12 oncogene (i.e., cancerous cells) to PCN_{DXR}-induced apoptosis.
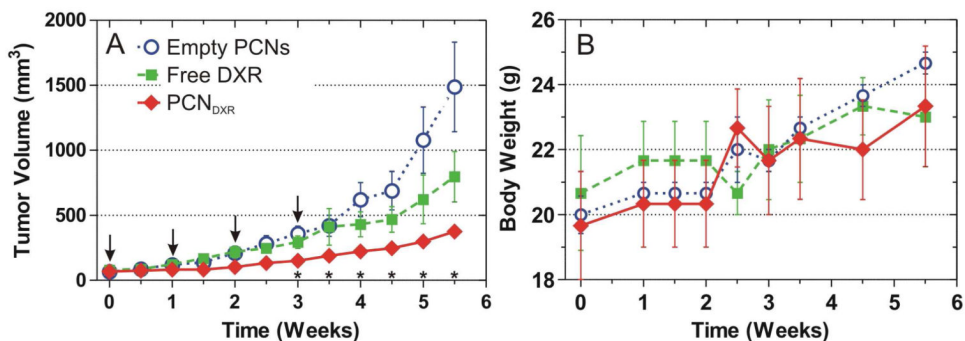
Figure 5.
In vivo antitumor effects of PCN$_{DXR}$, empty PCNs, or free DXR as administered by intraperitoneal injection to female nude mice bearing MDA-MB-231 human triple negative mammary tumors (n = 3 mice with bilateral tumors, 6 tumors per group). (A) Mean tumor volume. Pairwise tests were performed to assess statistical significance and were Bonferroni-corrected; * indicates $p < 0.05$ for PCN$_{DXR}$ compared with empty PCNs. PCN$_{DXR}$ was also significantly different from free DXR on weeks 1.5 and 2.5 (not shown in plot). Times of treatments are indicated by arrows (*points*, raw mean; *error bars*, standard error). (B) Body weights of each treatment group (*points*, mean; *error bars*, standard error).
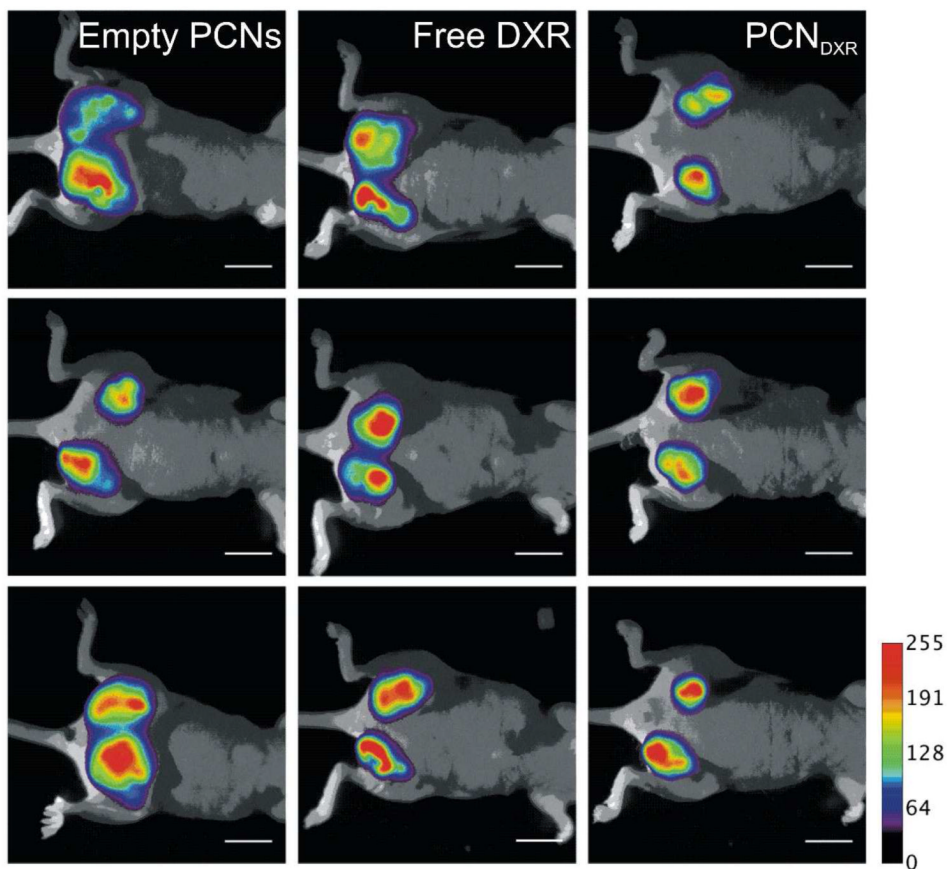
Figure 6.
Non-invasive fluorescent imaging of nude mice with mCherry-labeled MDA-MB-231 mammary tumors treated with empty PCNs, free DXR, or PCN_{DXR} (scale bar = 1 cm). mCherry fluorescence is pseudo-colored and overlaid over bright-field images. All members in each group are shown (n = 3 mice and 6 tumors).
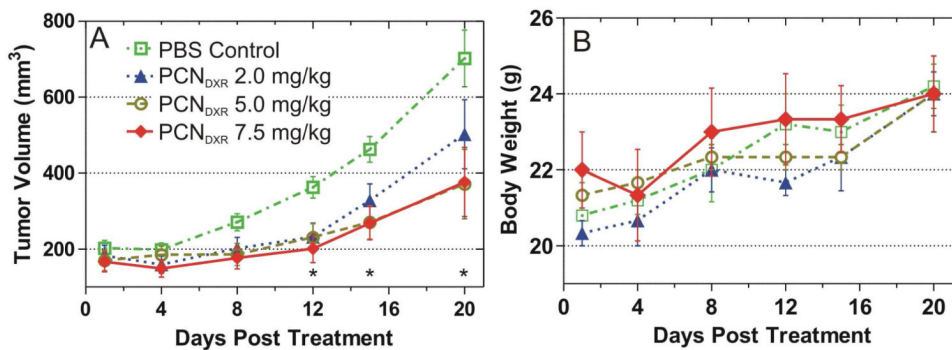
Figure 7.
In vivo antitumor effects of PCN_{DXR} (2.0, 5.0, or 7.5 mg/kg of DXR) administered by intraperitoneal injection to female nude mice bearing MDA-MB-231 mammary tumors (n = 3 mice with bilateral tumors, 6 tumors per group). (A) Mean tumor volume. Pairwise tests were performed to assess statistical significance and were Bonferroni-corrected; * indicates $p < 0.05$ for PCN_{DXR} doses 5.0 and 7.5 mg DXR/kg compared with PBS (*points*, raw mean; *error bars*, standard error). PCN_{DXR} at 2.0 mg DXR/kg dose was also statistically different on days 12 and 15 (not shown in plot). (B) Body weights of mice in each treatment group (*points*, mean; *error bars*, standard error).

Table 1

Half maximal inhibitory concentrations (IC_{50}/$\mu g \cdot mL^{-1}$; mean ± standard deviation) of PCN_{DXR}, free DXR and BL_{DXR}.

Drug Formulation	Exposure Time	IC_{50} (µg/mL)	
		MDA-MB-231	**HeLa**
PCN_{DXR}	48 h	29.6 ± 7.7	21.3 ± 6.4
	72 h	6.2 ± 1.2	5.5 ± 0.6
Free DXR	48 h	8.4 ± 1.4	1.5 ± 0.2
	72 h	1.4 ± 0.7	0.4 ± 0.1
BL_{DXR}	48 h	13.8 ± 4.9	13.0 ± 1.9
	72 h	3.8 ± 1.1	3.8 ± 0.4
Empty PCNs	72 h	non-toxic	non-toxic